PERGAMON

Vision Research 41 (2001) 495–505

Vision Research

www.elsevier.com/locate/visres

Effect of light sleep on three-dimensional eye position in static roll and pitch

J.H. Cabungcal [a,*], H. Misslisch [a], H. Scherberger [b], K. Hepp [c], B.J.M. Hess [a]

[a] *Department of Neurology, University Hospital of Zurich, Frauenklinikstrasse 26, 8091 Zurich, Switzerland*
[b] *Division of Biology, CALTECH, Pasadena, CA, USA*
[c] *Institute for Theoretical Physics, ETH Zurich, 8093 Zurich, Switzerland*

Received 29 May 2000; received in revised form 31 July 2000

Abstract

We examined three-dimensional eye positions in alertness and light sleep when monkeys were placed in different roll and pitch body orientations. In alertness, eye positions were confined to a fronto-parallel (Listing's) plane, torsional variability was small and static roll or pitch induced a torsional shift or vertical rotation of these planes. In light sleep, the planes rotated temporally by about 10°, torsional variability increased by a factor of two and the static otolith-ocular reflexes were reduced by about 70%. These data support the importance of a neural control of the thickness and orientation of Listing's plane, and suggest that part of the vestibular input underlying otolith-ocular reflexes depend on polysynaptic neural processing.

Keywords: Eye movement; Ocular torsion; Otolith; Listing's law; Sleep

1. Introduction

Since Helmholtz (1867) it is known that the brain selects a two-dimensional subgroup from among the range of mechanically possible three-dimensional (3D) eye positions, a finding called Listing's law. This law states that 3D eye positions are confined to a single plane — when the head is upright and stationary and eye positions are expressed as rotation vectors relative to a common reference position. When primary position is chosen as reference, i.e. when data are represented in Listing's coordinates, the plane of eye positions is called Listing's plane (LP). Previous work in alert monkeys and humans has shown that Listing's law holds during saccades, fixations, smooth pursuit (Tweed & Vilis, 1990; Haslwanter, Straumann, Hess, & Henn, 1992; Tweed, Fetter, Andreadaki, Koenig, & Dichgans, 1992) and, in a generalized sense, during vergence (humans: e.g. Mok, Ro, Cadera, Crawford, & Vilis, (1992); Minken & van Gisbergen, 1994; monkeys: Misslisch & Hess, 1999) but can be violated by the rotational vestibulo-ocular reflex (humans: Misslisch, Tweed, Fetter, Sievering, & Koenig, 1994; monkeys: Angelaki & Hess, 1996; Misslisch & Hess, 2000). A large range of ocular torsion in violation of Listing's law has also been observed in sleep (Nakayama, 1975; Suzuki, Kase, Kato, & Fukushima, 1997) leading to the proposal that Listing's law is the consequence of active neural rather than passive mechanical constraints.

Previous studies on static otolith-ocular reflexes have shown that 3D eye positions still lie in Listing's plane but that this plane is shifted along the torsional axis in roll and tilted around the vertical axis in pitch (Crawford & Vilis, 1991; Haslwanter et al., 1992). With a gain of about 0.10, these ocular counterroll and counterpitch responses, measured in alert monkeys, were relatively low. The effect of light sleep on the orientation of Listing's plane in small body roll orientations has been determined by Suzuki et al., (1997). They reported that the ocular counterroll observed in alert animals was reduced by about 50% in drowsiness. Controversial results have been reported on the effects of lesioning the vertical-torsional neural integrator in the interstitial nucleus of Cajal (iNC) on ocular counterroll. Whereas

* Corresponding author. Tel.: +41-1-2555500; fax: +41-1-2554507.
E-mail address: cabungcal@nos.usz.ch (J.H. Cabungcal).

0042-6989/01/$ - see front matter
PII: S0042-6989(00)00279-0

Crawford and Vilis (1999) reported the absence of a shift in Listing's plane, i.e. a complete disappearance of counterroll after the postsaccadic eye drift settled, Helmchen, Rambold, Fuhry, and Büttner (1998) found that counterroll was preserved. Crawford and Vilis (1999) suggested that ocular counterroll is produced by phasic otolith signals sent to the 3D neural integrator, which controls the orientation of Listing's plane. If this conclusion were correct, inactivating the vertical-torsional integrator would have to result in canceling the effect of gravity on the orientation of Listing's plane. To date, no reports exist on the effects of sleep or iNC lesions on the vertical orientation of Listing's plane (due to ocular counterpitch).

In this study, we re-examined the gravity-dependent orientation of Listing's plane in alertness and light sleep in upright and ten static roll ($-100°$, $-80°$,… $100°$) and ten static pitch ($-100°$, $-80°$,… $100°$) orientations. In light sleep we found a striking decrease of otolith-ocular reflexes, both in roll and pitch, as well as an increase in the range of ocular torsion.

2. Methods

2.1. Preparation of animals

Experiments were performed on four juvenile rhesus monkeys (Macaca mulatta; abbreviated ME, JU, SU, RO) weighing between 3.5 and 4.5 kg. The animals were chronically prepared for 3D eye movement recordings. Using sterile surgical techniques, skull bolts for head restraint and a dual search coil were implanted under inhalative anesthesia with a mixture of O_2–N_2O and further supplemented with halothane, if required, to maintain a constant level of anesthesia. In one animal, a recording chamber was stereotaxically implanted over a trephine hole for single-neuron recordings in the riMLF and PPRF as previously described (Henn, Baloh, & Hepp, 1984; Suzuki, Büttner-Ennever, Straumann, Hepp, Hess, & Henn, 1995). After surgery, animals were treated with antibiotics and analgesics. All procedures were in accordance with the NIH Guide for the Care and Use of Laboratory Animals, and the Veterinary Office of the Canton of Zürich approved the protocol.

2.2. Measurement, calibration and representation of 3D eye position

3D positions of the right eye were measured with the magnetic field-search coil technique using an eye position meter 3000 (Skalar Instruments, Delft, The Netherlands). Calibration of eye position data was carried out as described in detail by Hess, van Opstal, Straumann, and Hepp (1992). Briefly, in an in-vitro procedure, the magnitude of the two coil sensitivity vectors as well as the angle between them was computed. In an in-vivo procedure, performed before each experiment, the animal repeatedly fixated three light emitting diodes placed either straight ahead, 20° down or 20° up, at a distance of 0.8 m. The voltages measured for these fixations were used together with the in-vitro determined coil parameters to compute offset voltages as well as the orientation of the search coil on the eye.

Eye positions were expressed as rotation vectors (Haustein, 1989) in a right-handed Cartesian coordinate system, determined by three head-fixed orthogonal axes: x-, y- and z-axis pointing forward, leftward and upward. According to the right-hand rule, positive x-, y- and z-components of the rotation vector correspond to clockwise, downward and leftward components of eye position. In the figures, the components of eye positions will be given in degrees.

2.3. Experimental setup and protocol

Animals were seated in a primate chair and secured with chair-fixed shoulder and lap belts. The head was restrained in a 15° nose-down position such that the lateral semicircular canals were approximately earth-horizontal (Böhmer, Henn, & Suzuki, 1985). The primate chair was placed inside the 3D vestibular rotator with three motor-driven axes (Acutronic, Jona, Switzerland). The accuracy of the position control on each axis was $<0.1°$. A lightproof sphere of 0.8 m radius surrounded the rotator enabling recordings in complete darkness.

During the experiments, the animals were initially positioned in upright and then rolled or pitched into ten different static positions in steps of $\pm 20°$. Spontaneous eye movements were recorded in each of the ten static roll and ten static pitch positions for the alert and light sleep condition. In alert trials (in the light), the experimenter drew the monkey's attention to various targets in the visual field to ensure that the animal made eye movements all over its oculomotor range. For comparison, we recorded a few trials in alert animals in darkness while applying auditory stimuli at various locations to induce eye movements over a wide range. When the animal was left for about 5 min in total darkness it fell into a light sleep state, determined by loss of all rapid eye movements as described below. Each eye movement recording consisted of 92 s of saccadic and fixational (alert) or drifting and oscillating (light sleep) eye movements. We usually recorded between 2 and 6 files per animal for each roll and pitch position, both in alertness and in light sleep.

2.4. Characteristics of three-dimensional eye movements in light sleep

When alert monkeys scan their visual environment they normally make three to four rapid eye movements per second to redirect their gaze line on objects of interest. In between these saccades lie periods of steady fixations in which these objects are visually inspected (Fig. 1A, torsional, vertical and horizontal eye position traces labeled 'E_x', 'E_y', and 'E_z', respectively). When alert animals made eye movements in darkness, the periods of steady fixations were prolonged (Fig. 1B). In agreement with previous studies (Henn, Baloh, & Hepp, 1984; Kuhlo & Lehman, 1964), we found that light sleep periods were characterized by the absence of the normal saccade-fixation pattern and the appearance of drifting eye movements and pendular eye oscillations at frequencies between about 0.2 to 0.3 Hz (Fig. 1C and D). To obtain a physiological correlate of the state of alertness, we measured the activity of premotor saccadic burst neurons in the two distinct periods of eye motion observed during alertness and light sleep in one monkey (Henn et al., 1984). More specifically, neurons in the rostral interstitial medial longitudinal fasciculus (riMLF) and the paramedian pontine reticular formation (PPRF) were recorded using tungsten electrodes (impedance 1.5–2 MΩ; Frederick Hare, USA). Activity in the riMLF was associated with the onset of vertical and/or torsional rapid eye movements (short-lead burst neurons), whereas discharges in the PPRF coded for ipsi-horizontal/ipsi-torsional saccades. When we recorded from the alert monkey in the light we obtained a typical pattern of short bursts of activity before and during a saccade in the neuron's on-direction followed by a silent period during the subsequent steady fixation (Fig. 1A, lower trace). We found a similar pattern in the alert animal in darkness although here the silent periods were prolonged due to extended fixation periods (Fig. 1B, lower trace). The normal discharge pattern alternating between short bursts and longer inactive periods was replaced in light sleep recordings by a continuous high-frequency discharge (between 50–200 Hz), which was presumably due to the lack of inhibition signals from pontine omnipause neurons (see Fig. 1C and D; Henn et al., 1984). Note that the first saccade occurring during the sleep-wake transition brought torsional eye position back to zero, i.e. corrected for the torsional deviations from Listing's law (Fig. 1C, arrow). In long periods of light sleep, large torsional eye position drifts could be observed (Fig. 1D). As in Fig. 1C and D we usually recorded light sleep data in darkness but in a few cases we recorded data in light and found eye movements with the same characteristics (drifts, oscillations). Occasionally, short periods of stable fixation or saccadic eye movements indicating alertness occurred within longer periods of drifting eye movements. We removed these 'alert' periods from the data traces collected in light sleep so that a typical light sleep trial contained between 50 and 70 s of slow eye movement data.

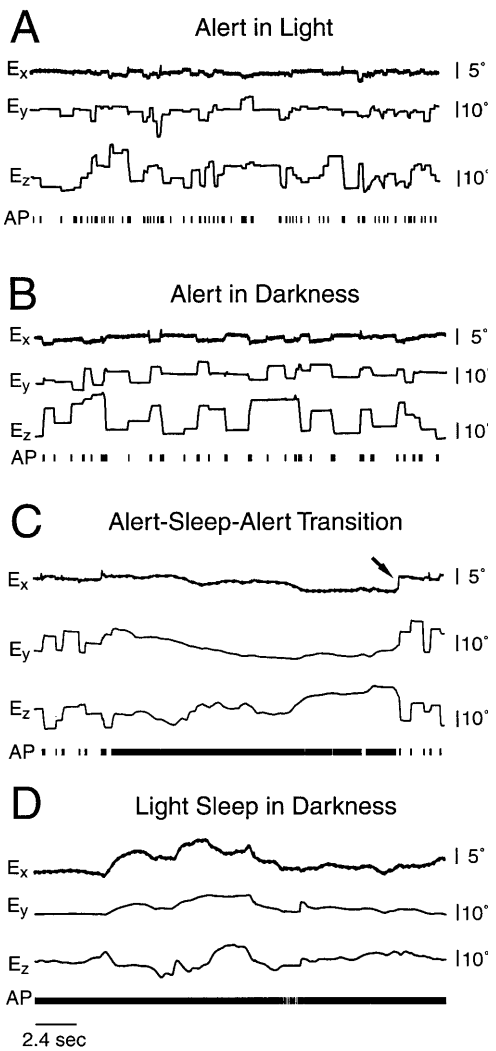

Fig. 1. Examples of 3D eye position and riMLF short-lead burst neuron recording in upright body orientation. (A) Spontaneous eye movements of alert monkey in a lighted environment. The neuron discharged briskly before and during saccades and was silent during fixations. (B) Fewer saccades due to prolonged fixations of alert monkey in darkness. (C, D) Slow drifts and oscillating eye movements during light sleep in darkness were accompanied by a continuous neuronal discharge that was only briefly interrupted in periods of steady fixation. Note the reset of torsional eye position achieved by the first saccade after a sleep period (arrow in C). E_x, E_y and E_z represent the torsional, vertical and horizontal component of eye position. The vertical lines denote action potentials (AP). Note that due to the low temporal resolution these lines may form clusters that actually include several APs. Note different scale of torsional eye position. Monkey ME.

2.5. Data analysis

For analysis of the drifting and slowly oscillating eye movements observed in light sleep, we used an interac-

tive computer program to remove periods where rapid eye movements or steady fixations occurred. That is, the program automatically eliminated periods where the eyes moved with large velocity (above 200°/s: saccades) or remained stable (below 5°/s: fixations) and kept those periods where the eyes moved with low velocity (below 100°/s: drift). As mentioned above, in one monkey we used the firing rate of short-lead burst neurons in the riMLF or PPRF to assist in the evaluation of light sleep periods. For light sleep data, only those eye position recordings extending more than about 15° in vertical and horizontal direction and lasting longer than 40 s were used to determine the orientation of the best-fit plane in various head positions.

We used 3D eye position data collected in alertness (saccades, fixations, smooth pursuit, blinks) and light sleep (slowly drifting and oscillating eye movements) to compute Listing's plane at the beginning of each experiment. First, by applying linear regression we determined the orientation of Listing's plane in the alert monkey when placed in an upright position. Second, we transformed the 3D eye position data into Listing's coordinates. Third, we computed the best-fit plane to eye positions recorded in different static head orientations by describing the torsional component of eye position as a function of vertical and horizontal eye position:

$$E_x = a_0 + a_1 E_y + a_2 E_z \quad (1)$$

where E_x, E_y, and E_z are torsional, vertical and horizontal components of eye position, a_0 is the shift of LP along the x-axis (torsional offset), a_1 determines the orientation of LP relative to the y-axis (y-slope: horizontal plane rotation) and a_2 represents the orientation of LP relative to the z-axis (z-slope: vertical plane rotation). As a measure of torsional eye position variability we computed the S.D. of the data from the best-fit plane along the x-axis ('thickness' of LP).

3. Results

We found that: (1) gravity-induced changes on 3D eye positions (ocular counterroll and counterpitch) are highly reduced in light sleep, (2) eye positions lie in horizontally rotated planes and (3) the range of torsional eye position was largely increased.

3.1. Characteristics of eye position planes during static roll

When an alert monkey is placed in a static roll position, the plane fitted to the 3D eye positions sampled during saccades and steady fixations are (torsionally) shifted along the x-axis, as first shown by Crawford and Vilis (1991) and Haslwanter et al. (1992).

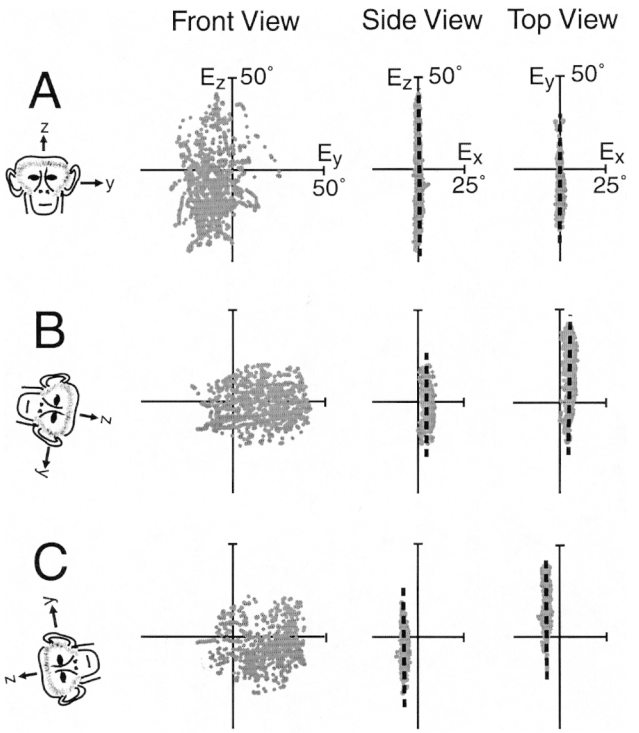

Fig. 2. Static body roll induced a moderate torsional shift of Listing's plane in the alert monkey. (A) 3D eye position vectors sampled during saccades and fixations in upright body position (gray data points) were confined to the fronto-parallel Listing's plane (side and top view). (B) Shift of Listing's plane along the positive x-axis (by 4.4° clockwise, CW) during counterclockwise (CCW) body orientation (100° left-ear down). (C) Shift of Listing's plane (by 7.1°) along the negative (CCW) x-axis during CW body orientation (100° right-ear down). In all orientations, the plane of eye position was parallel to the y-axis (top view) indicating that the horizontal tilt of Listing's plane was close to zero (0.0°, −0.2° and −1.2° in A–C) and the width of Listing's plane (the torsional standard deviation of all eye positions from the best-fit plane) was 0.7°, 1.5° and 1.1° (A–C), respectively. Data were recorded during 92 s of spontaneous eye movements in the light. Monkey ME.

Fig. 2 shows examples of 3D eye position data collected in an alert animal in upright (A), 100° left-ear down (B) and 100° right-ear down (C) body orientations. To reveal the 3D arrangement of the data and the best-fitted planes, we plotted the different components of eye position in three views: horizontal versus vertical (left column labeled 'front view'), horizontal versus torsional (middle column labeled 'side view') and vertical versus torsional (right column labeled 'top view'). Inspecting Fig. 2A shows that eye rotation vectors for saccades and steady fixations in upright body position cover a large horizontal (data points along the ordinate) and somewhat smaller vertical (data points along the abscissa) range. Plotting the same data points in side and top views illustrates the planar organization of the eye position data, i.e. the torsional components of the eye rotation vector are close to zero when plotted in the Listing coordinates shown. When the monkey is

placed at 100° left-ear down (counterclockwise; Fig. 2B), the data still lie in a plane (dashed lines in side and top views), but one that is shifted along the abscissa of the side and top view. The shift in the positive torsional direction means that the counterclockwise head orientation induces clockwise torsional eye position components that accompany any combination of horizontal (side view) and/or vertical (top view) eye position. A similar pattern is observed when the monkey is placed in a 100° right-ear down (clockwise) position, but now the shift of Listing's plane is in the opposite direction inducing constant counterclockwise eye position components. That is, static head roll induces low-gain ocular counterroll.

What happens to the ocular counterroll in periods of light sleep? To examine this point we plotted, in the same views and for the same roll positions as in Fig. 2, examples of 3D eye positions collected during slowly drifting and oscillating eye movements (Fig. 3). From inspecting the plots, three observations can be made:

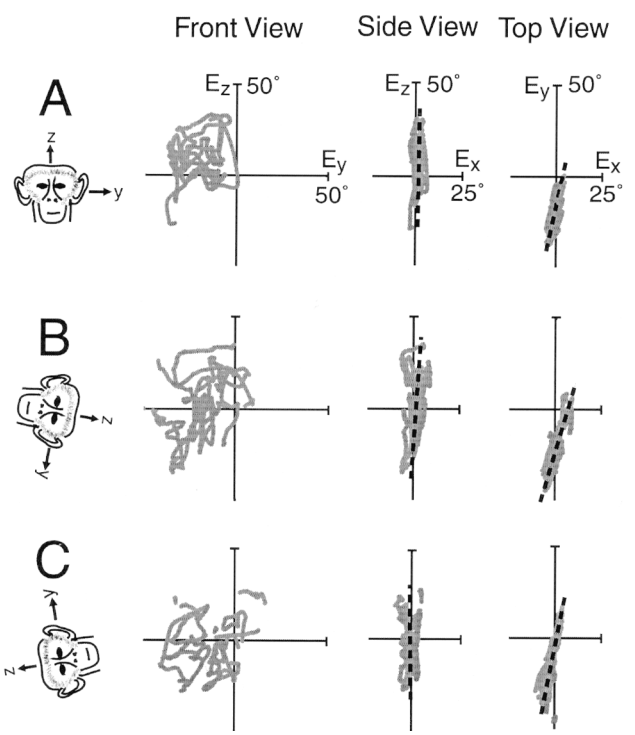

Fig. 3. The roll-dependent torsional shift of the best-fit eye position plane was considerably reduced in light sleep. (A) Tips of 3D eye position vectors collected during slow drifts and oscillations in upright body orientation (gray data) showed a large increase in the range of torsional eye positions (side and top view) indicating a violation of Listing's law. (B, C) The best-fit planes showed only a small torsional offset (1.5° CW/ − 1.1° CCW) opposite to the direction of body tilt (100° CCW/100° CW). Independent of body roll, the best-fit planes were considerably rotated (around the z-axis) to the right by − 6.8, − 13.5 and − 11.9° (A–C). The width of the best-fit eye position planes was 1.3, 1.8 and 1.7°, respectively (A–C). Data consisted of 60, 69 and 60 s of slow drifts and oscillations (A–C). Same format and views as in Fig. 2. Monkey ME.

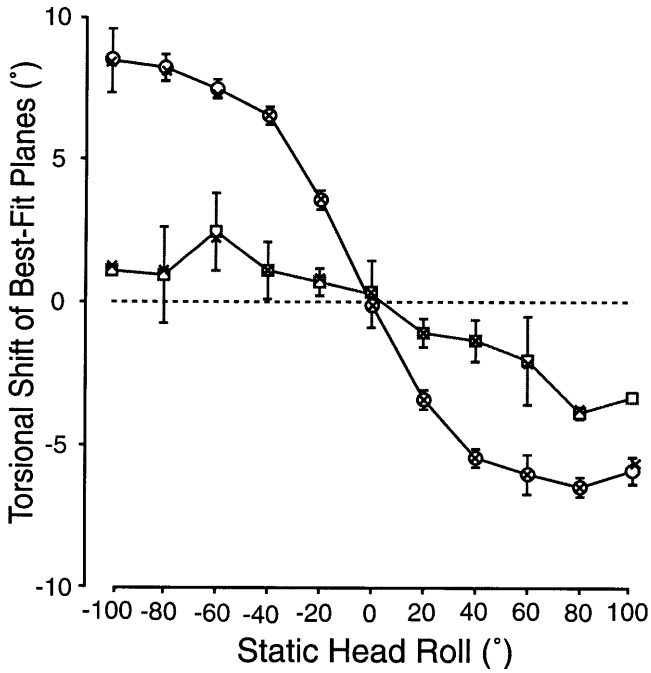

Fig. 4. Example of ocular counterroll during static head roll. The shift of the planes fitted to the 3D eye position data in alertness (circles) was markedly reduced in light sleep (squares), averaged over all roll orientations by 70.0%. Values are means of repeated measurements, the vertical bars (alert/sleep) denote ± S.D. The mean values derived from 100 repeated fits performed by bootstrap analysis (crosses) were very close to the data derived from the best-fit planes confirming the robustness of the fit procedure. Monkey SU.

(1) compared to its value obtained in alertness, the shift of the best-fit planes in ear-down positions was considerably reduced; (2) the planes tilted by large amounts horizontally, towards the side of the recorded eye (i.e. temporally), in all roll positions; (3) relative to the alert data, torsional variability increased-in particular for the ear-down positions.

We quantified the shift of the best-fit planes for all static head roll positions and for alertness and light sleep data by linear regression (see Section 2). To assess the statistical reliability of the fit procedure, we applied a bootstrap analysis (Efron & Tibshirani, 1993; Press, Teukolsky, Vetterling, & Flannery, 1992) on a complete data set obtained in one animal. As can be seen in Fig. 4, the mean values for the torsional shift of the best-fit Listing planes in alertness (circles, ± S.D. indicated by vertical bars) and light sleep (squares, ± S.D. indicated by vertical bars) were well reproduced by bootstrap analysis (crosses). More specifically, in each roll position and for each wake state data were collected between two and six times. Then, for each data set, we applied the bootstrap analysis, yielding the mean torsional shift from 100 synthetic data sets obtained by drawing random samples with replacement from the experimentally measured values (see e.g. Press et al., 1992). The crosses in Fig. 4 denote the overall average

of the bootstrap values for a given roll position. The standard deviations from the bootstrap mean were negligible (in Fig. 4, they were invariantly smaller than the vertical extension of the crosses), demonstrating that the fit procedure was robust.

Fig. 4 demonstrates that the torsional shift of LP is clearly modulated by static head roll when the animal is alert (maximum torsional shift about 8° when the head is tilted −100°, i.e. counterclockwise) and that this modulation is considerably diminished in light sleep (by 70% when averaged over all roll positions). This pattern was observed in all four animals as summarized in Fig. 5 that compares the mean torsional shift of the best-fit eye position plane (averaged over all trials in all animals) for all roll positions in alertness (circles) and light sleep (squares). As in Fig. 4, vertical bars for both alert and light sleep indicate the standard deviation from the means. The torsional shift of the best-fit planes in light sleep was more variable and significantly lower than the corresponding alert values (student t-test, $P < 0.05$; filled symbols) except at upright body orientation where both conditions yielded close to zero values. Averaged over all roll positions ocular counterroll observed in alertness was reduced by 66.5% in light sleep (range 50.0 to 96.1%).

As mentioned above, another consistent result, found in all (128) trials of all four animals, was the large horizontal rotation of the fitted planes. Fig. 6 illustrates that the average (all trials at a given static roll position, all animals) horizontal rotation of the best-fit planes differed considerably for data obtained in alertness (circles, ±S.D.) or in light sleep (squares, ±S.D.). Except for the −60° roll position we did not observe a significant horizontal rotation for the alert data (t-test, $P < 0.05$). On the other hand, we did find large mean tilt angles ranging from −8.6 to −17.6° for the light sleep data. The negative sign indicates that the planes computed for the data recorded for the right eye invariantly rotated to the right, i.e. the planes rotated temporally. The amount of temporal plane rotation did not depend on head roll (one-way ANOVA, $F(10,118) = 3.64$, $P < 0.0003$).

A third observation, clearly visible in the example of Fig. 3 (side and top views), was that the range of ocular torsion, i.e. the 'thickness' of the best-fit plane depended on the body's roll orientation in alertness, increasing with increasing roll angles (t-test, $P < 0.05$). During light sleep, it increased even further in most static roll positions (Fig. 7, light sleep data: squares; alert data: circles). For example, in the upright position the standard deviation from the best-fit planes was 0.7° averaged over all experiments in alertness (S.D. ±0.1, $n = 16$) and 1.5° in light sleep (S.D. ±0.8, $n = 19$). The large increase of torsional variability and the large temporal rotations of the best-fit planes represent a clear violation of Listing's law in light sleep.

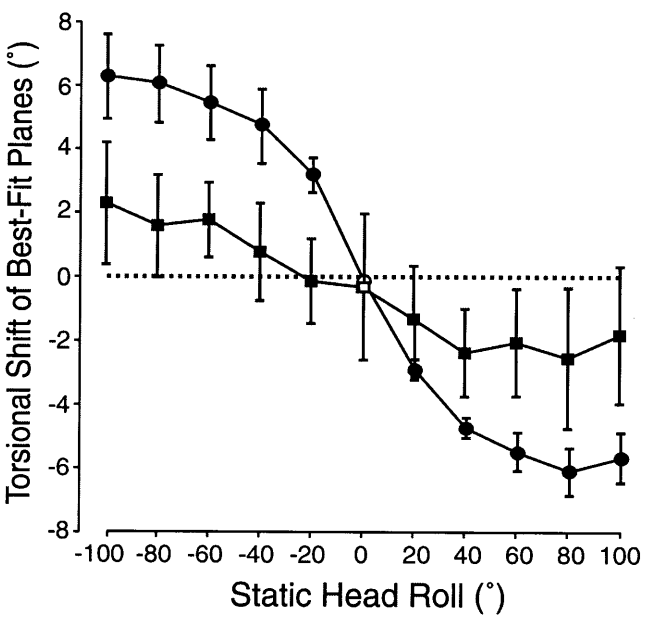

Fig. 5. Quantitative analysis of ocular counterroll in alertness and light sleep. The torsional shift of the planes fitted to 3D eye positions was considerably reduced in light sleep (squares) compared to alertness (circles). Values are means over all experiments in all four animals.

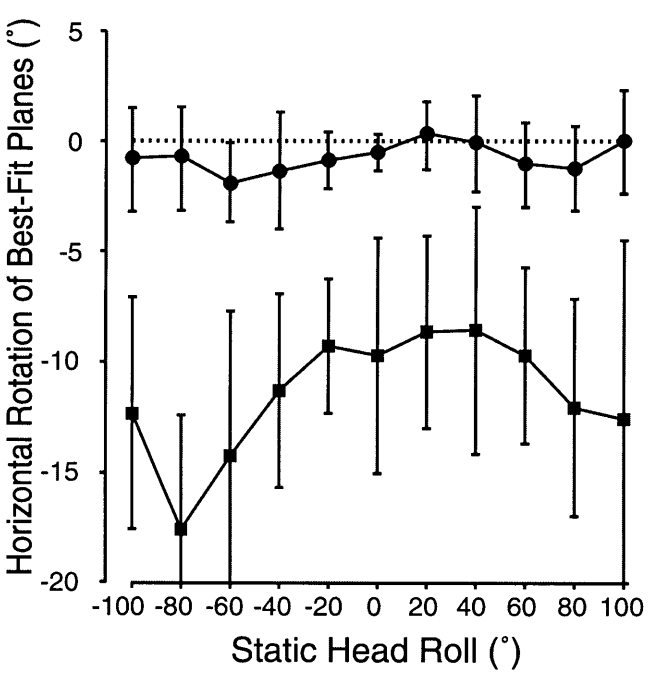

Fig. 6. Large horizontal rotation of best-fit eye position planes during static head roll in light sleep. Horizontal tilt angles were close to zero for saccade and fixation data obtained in alertness (circles) but prominent in light sleep (squares) for all roll orientations (mean: −11.3°, range: −8.6–−17.6°). Negative values indicate that the planes rotated rightward. Data that were significantly different (t-test, $P < 0.05$) during alertness and light sleep are represented by filled symbols.

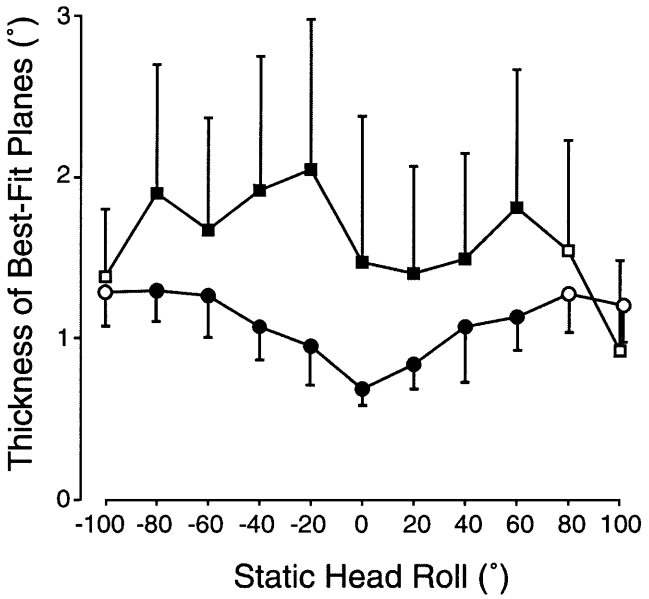

Fig. 7. Width (thickness) of eye position planes in static roll orientations. In the alert animal, the width of the plane fitted to saccadic and fixational eye positions was larger in more eccentric roll positions (circles). The width of the plane fitted to drifting eye position data increased in light sleep except at extreme roll positions (squares). Statistical differences (t-test, $P < 0.05$) are denoted by filled symbols.

3.2. Characteristics of eye position planes during static pitch

When an alert monkey is placed in a static pitch position, the plane fitted to the 3D eye positions is vertically rotated around the y-axis (Fig. 8), as described earlier by Crawford and Vilis (1991) and Haslwanter et al. (1992). The figure shows, in the same format as in Fig. 2, eye position data collected in an alert animal in different body orientations (see cartoon heads). In the upright position (A) the rotation vectors show a planar organization and are confined to an almost fronto-parallel plane (dashed lines in side and top view). This plane is tilted somewhat down in nose-up pitch (B, side view) and up in nose-down pitch (C, side view) indicating that Listing's plane tilts opposite to the head tilt albeit with low gain. In other words, ocular counterpitch is insignificant in sleep.

The vertical orientation of the planes fitted to the slow drifting eye movements in light sleep did not depend on head pitch. In Fig. 9, the best-fit plane was rotated slightly upward (away from the E_z-axis) when the animal was in an upright body orientation (side view, top panel), but was approximately aligned with the z-axis in 100° nose-up/nose-down orientations (side view, middle/bottom panels). In other words, body pitch did not systematically influence the vertical orientation of the best-fit plane. And as in the roll case, the best-fit planes in all pitch orientations were rotated horizontally (top view), and torsional variability was largely increased (side view).

Fig. 10 summarizes the mean vertical rotation of the best-fit planes (averages over all trials and all monkeys) for data obtained in alertness (circles, vertical bars are $\pm$S.D.) and light sleep (squares, bars denote $\pm$S.D.). While alert, the vertical rotation of the fitted planes is a function of head pitch that peaks at ± 80–$100°$ static pitch orientation. In light sleep, the vertical orientation of the best-fit planes is no longer modulated by body pitch but shows a mean offset of $-2.8°$, i.e. the planes are rotated slightly upward. Corrected for the offset, the modulation observed during alertness was reduced on average by 74.5%.

The horizontal orientations of the best-fit planes obtained in alertness were very unlike those obtained in light sleep. Fig. 11 plots the average (all trials, all animals) horizontal rotation for data obtained in alertness (circles, vertical bars indicate $\pm$S.D.) and light sleep (squares, bars denote $\pm$S.D.) data. The angles of horizontal plane rotation computed for the alert data were very small and, except for the 40 and 60° (nose-

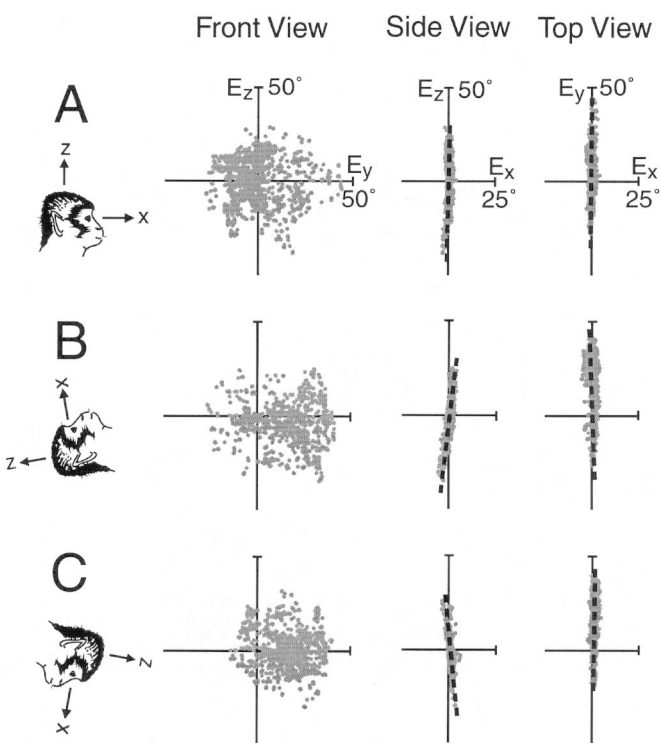

Fig. 8. Static body pitch elicited a moderate vertical rotation of Listing's plane in the alert monkey. (A) 3D eye positions during saccades and fixations in upright body position lay in Listing's plane, which is parallel to both the z- and y-axes. (B) Vertical rotation (6.9° down) in $-100°$ nose-up orientation. (C) Vertical rotation ($-3.6°$ up) in 100° nose-down orientation. Only minor horizontal rotations of Listing's plane were observed (-0.2, 1.1 and $-0.8°$ in A–C). The width of the fitted (Listing's) plane was 0.7, 0.9 and 0.7° (A–C). Same format and views as in Figs. 2 and 3. Monkey ME.

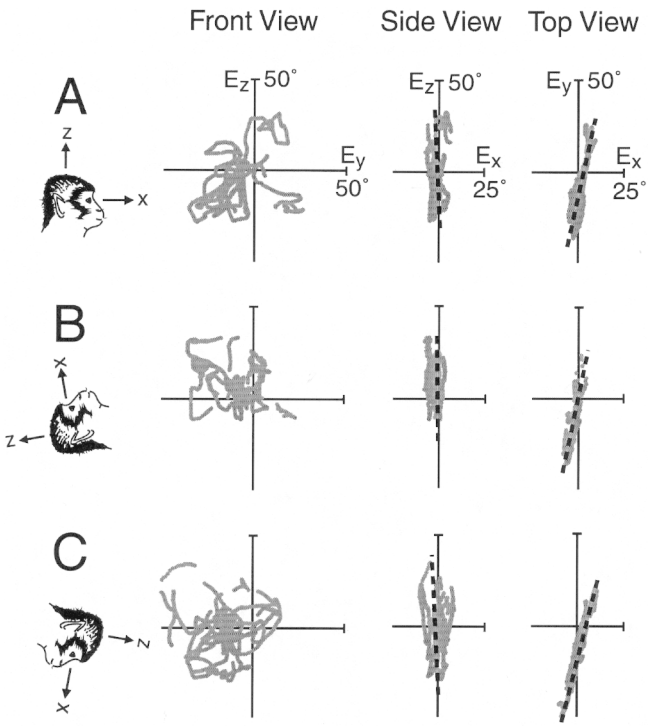

Fig. 9. The pitch-dependent vertical tilt of the best-fit plane was greatly reduced in light sleep. (A) 3D eye position vectors during slow drifts in upright body position (gray data points) lay in a plane that was almost parallel to the z-axis (tilted by $-0.7°$ up). (B, C) The eye position planes did not systematically tilt during $-100°$ nose-up (plane tilt of $-2.0°$, in non-compensatory direction) and 100° nose-down (plane tilt of $-1.2°$) pitch. In all examples, the best-fit planes showed large horizontal tilts (-9.4, -9.0 and $-13.5°$ in A–C) and a large scatter of ocular torsion (plane width of 1.6, 1.1 and 1.1° in A–C) suggesting a clear deviation from Listing's law. Same format and views as in Figs. 2, 3 and 8. Monkey ME.

down) pitch positions, not significantly different from zero (t-test, $P < 0.05$). Large negative values (mean: $-10.5°$, range: -9.0–$-13.5°$) were seen for the slow drift eye position planes obtained during light sleep. The amount of horizontal (temporal) plane rotation did not depend on head pitch (one-way ANOVA, $F(10,175) = 3.68$, $P < 0.0009$).

As in the roll case torsional variability was increased during drifting eye movements, rising from an average (all trials, all monkeys) of 0.7° (± 0.1, $n = 119$) in alertness to 1.5° (± 0.2, $n = 179$) in light sleep (Fig. 12). Taken together, the data obtained in static pitch positions confirmed the data obtained in roll positions in that otolith-ocular reflexes and Listing's law break down in the transition from alertness to sleep.

4. Discussion

We examined the effects of the state of alertness on 3D eye positions in static roll and pitch body orientations. In light sleep, we found a large reduction of ocular counterroll and counterpitch, large temporal rotations of the eye position planes, and a large increase of the range of ocular torsion.

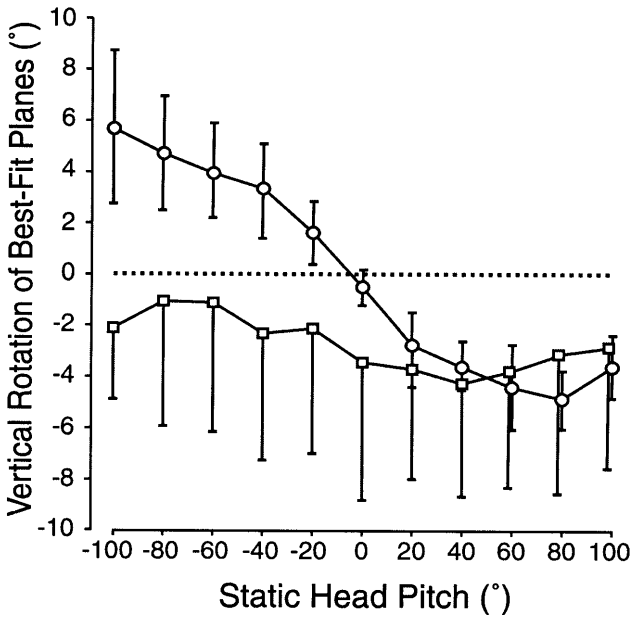

Fig. 10. Quantitative analysis of ocular counterpitch in alertness and light sleep. Compared to their value in alertness (circles), the vertical tilt of the best-fit planes was greatly reduced in light sleep (squares) and showed a negative offset (i.e. the planes were usually rotated upward from the positive z-axis). Values are means over all trials in all animals.

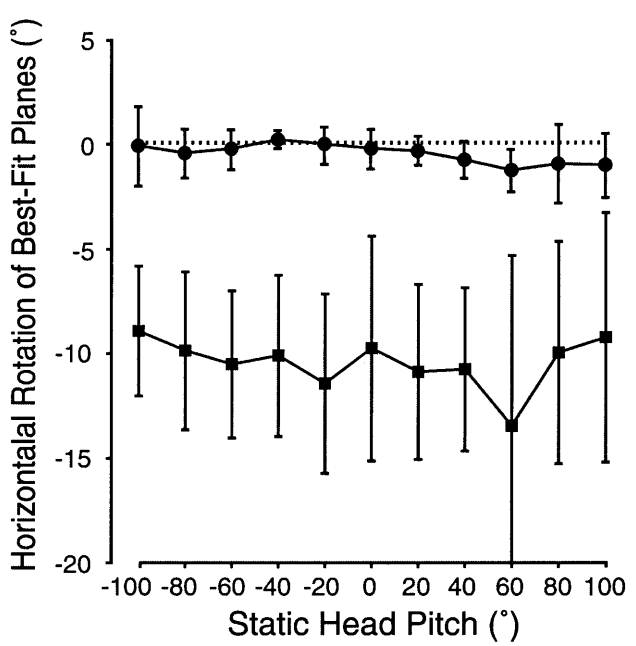

Fig. 11. Large horizontal rotation of best-fit eye position planes during static head pitch in light sleep. As in roll (Fig. 6), data collected in the alert monkey (circles) showed almost zero horizontal rotation angles. Large negative values were observed in light sleep (circles) and in all pitch orientations (mean: $-10.5°$, range: -9.0–$-13.5°$).

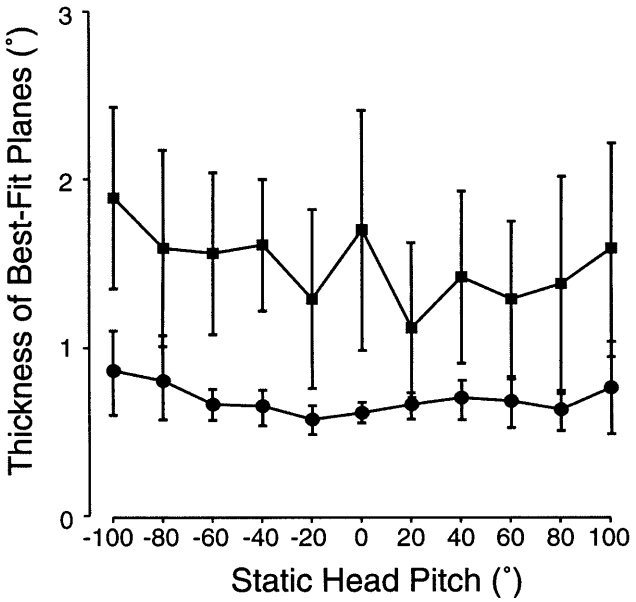

Fig. 12. Width (thickness) of eye position planes in static pitch positions. For data sampled in alertness (circles), the width of the best-fit (Listing's) plane increased in some eccentric pitch positions (-100, -80, 40 and 100°, t-test, $P < 0.05$). In light sleep (squares), plane thickness was significantly larger than the alert values in all pitch positions (t-test, $P < 0.05$; filled symbols).

4.1. Changes in the geometric constraints on 3D eye positions in alertness and light sleep

In the alert monkey, 3D saccadic and fixational eye positions (expressed as rotation vectors) were confined to a fronto-parallel (Listing's) plane. The torsional deviation from that plane was small ($< 0.9°$) and agreed with earlier studies (Tweed & Vilis, 1990; Haslwanter et al., 1992). In light sleep, the normal saccade-fixation pattern was replaced by slow drifts and pendular eye oscillations. As a consequence, 3D eye positions deviated more from the best-fit plane as indicated by a large increase of torsional variability (Figs. 3, 7, 9 and 12). An even more serious deviation from Listing's law was the large horizontal rotation of the eye position planes observed in all light sleep trials, independent of the body's orientation with respect to gravity. Thus, 3D positions of the right eye lay only roughly in a plane and this plane was rotated to the right, away from alignment with the y-axis (Figs. 3, 6, 9 and 11). This temporal rotation means that in general downward/upward eye positions are associated with clockwise/counterclockwise torsion. A similar pattern (binocular extension of Listing's law, L2) has been described to hold for both eyes during vergence eye movements, with a close relation between temporal plane rotation and the vergence angle (e.g. Mok, et al., 1992; Minken & van Gisbergen, 1994; Bruno & van den Berg, 1997; Tweed 1997). Preliminary results from an ongoing study on the geometry of binocular eye positions in light sleep indicate the absence of such a systematic relationship, i.e. the temporal rotation of the two eye position planes is not a precise function of vergence angle as predicted by L2 (Cabungcal, Misslisch, Scherberger, Hepp, & Hess, 2000).

An extended range of ocular torsion by a factor of two has been mentioned by Suzuki et al. (1997), in the drowsy monkey, but they did not report quantitative data. After uni- and bilateral lesions of the torsional velocity-to-position integrator in the interstitial nucleus of Cajal (iNC), Helmchen et al. (1998) found that the width of Listing's plane raised from 1.4° to 2.2°, an increase of 63%. Likewise, Crawford, Cadera and Vilis (1991) reported that microstimulation or unilateral lesion of the iNC produced eye movements out of Listing's plane. We found that the appearance of drifting and oscillating eye movements in light sleep was accompanied by characteristic changes in the discharge of brainstem burst neurons involved in saccade generation (riMLF neuron in Fig. 1). This confirms previous studies that reported premotor burst neurons that lost their distinct burst pattern and showed continuous low-frequency firing in sleep (Henn et al., 1984; Raybourn & Keller, 1977). It is also known that omnipause neurons, constantly active except during saccadic periods in alertness, became entirely inactive in light sleep (Henn et al., 1984). Thus, the ongoing activity in the burst neurons most likely reflects the lack of systematic inhibition by the omnipause neurons that is normally observed in awake monkeys. In alertness, microstimulation or unilateral lesions of the torsional-vertical short-lead burst neurons in the riMLF induce eye movements out of Listing's plane (Henn, Straumann, Hess, Hepp, Vilis, & Reisine, 1991; Crawford & Vilis, 1992; Suzuki, Straumann, Hess, & Henn, 1994; Suzuki et al., 1995).

Small torsional deviations from Listing's plane are normally corrected by saccades that bring the eye position back into Listing's plane. Of course, this correction mechanism that has been found to involve the nucleus reticularis tegmenti pontis (van Opstal, Hepp, Suzuki, & Henn, 1996) was non-functional in light sleep: per definition, this period is characterized by slowly drifting, oscillating eye movements and by the absence of (torsion-correcting) saccades. Thus, we regularly found ocular torsion to adopt large values that were zeroed by the first saccade occurring in the sleep-wake transition (see Fig. 1C). Additional support for the idea of a cerebellar involvement in the maintenance of Listing's law has been reported by Straumann, Zee, & Solomon (2000) who found significant torsional eye position drifts in patients with cerebellar atrophy. Taken together, these findings suggest the importance of neural control mechanisms in the brainstem and cerebellum, which generate accurate rapid eye movements and steady fixations in the alert monkey and break down in light sleep,

resulting in deviations from close adherence to Listing's law. Of course, this does not mean that there are no mechanical factors in eye control. It is clear, however, that mechanical factors alone cannot explain our observed deviations from Listing's law: because passive plant mechanics would not change their effect on ocular kinematics when a subject's mental state changes from alertness to light sleep, the range of ocular torsion should be equal in alertness and in sleep, and there should be no temporal rotation of the eye position planes during light sleep. A combination of the two factors, plant mechanics and neural commands, has been suggested as an explanation of Listing's law, with muscle pulleys and related tissue defining Listing's plane and motor commands conforming to this setting (Demer et al., 1995; Miller & Demer, 1997). In the wake-sleep transition, then, either the stiffness in the extraocular rectus pulleys could be changed by smooth muscle innervations (Demer, Poukens, Miller, & Micevych, 1997), or the anterior-posterior location of the muscle pulleys could be changed by orbital layer rectus muscle fibers (Demer, Oh, & Poukens, 2000), resulting in an increase of torsional eye position variability. Note that both these possibilities would not work without neural control mechanisms. Thus, while no one argues against the need for neural commands, the exact role of plant mechanics in the implementation of Listing's law remains unclear. The finding of even another layer of extraocular muscle fibers (marginal zone, Wasicky, Ziya-Ghazvhini, Blumer, Lukas, & Mayr, 2000), whose functional significance is not yet understood, indicates that more work is needed to determine the mechanical properties of the oculomotor plant.

4.2. Ocular counterroll and counterpitch in alertness and light sleep

We found that static otolith-ocular reflexes modified the orientation of Listing's plane for saccades and fixations as reported previously (Haslwanter et al., 1992): a torsional shift during roll and a vertical rotation during pitch (Figs. 2, 4, 5, 8 and 10). In light sleep, the amount of torsional shift and vertical rotation of the cloud of 3D eye positions was clearly reduced (Figs. 3–5, 9 and 10). A dysfunctional neural integrator has been suggested as a possible cause of reduced ocular counterroll by Crawford & Vilis (1999). After lesions of the torsional velocity-to-position integrator located in the iNC, they found that ocular counterroll was entirely abolished after postsaccadic eye position drift had settled and concluded that ocular counterroll is produced by phasic otolith signals sent to the neural integrator (iNC). In contrast, Helmchen et al. (1998) (monkey) and Anderson (1981) (cat) found normal ocular counterroll after iNC lesions. Helmchen et al. (1998) suggested that the iNC is not involved in the generation of conjugate torsional eye positions during head roll. Rather, direct projections from vestibular nuclei neurons to the oculomotor nuclei through the MLF are believed to mediate this static otolith-ocular reflex (McCrea, Strassmann, & Highstein, 1987; Markham, 1989; Iwamoto, Kitama, & Yoshida, 1990). Our data, with counterroll and counterpitch responses reduced by about 70% in light sleep, cannot distinguish between these two alternatives. However, some information from the otoliths must reach the oculomotor nuclei to modify torsional eye position during roll and pitch even in light sleep. The relatively large variability in the obtained counterroll and counterpitch responses may indicate that otolith signals that bypass the velocity-to-position integrator and project directly to the oculomotor muscles are rather weak.

5. Conclusions

Compared to the alert animal, the modulation of 3D eye positions by roll and pitch was reduced by about 70% in light sleep. Furthermore, the best-fit planes rotated by about 10° temporally, and the range of ocular torsion increased by about 100%. These data suggest that normal static counterroll and counterpitch, as well as a close adherence to Listing's law, require coordinated and precise neural control mechanisms in the brainstem and cerebellum.

Acknowledgements

This work was supported by the Betty and David Koetser Foundation for Brain Research and a Swiss National Science Foundation grant to B.J.M.H. # 31-47287.96. We thank Bernadette Disler and Albert Züger who provided us excellent technical assistance and Drs Max Dürsteler and Daniel Forney for their excellent computer support.

References

Anderson, J. H. (1981). Ocular torsion in the cat after lesions of the interstitial nucleus of Cajal. *Annals New York Academy of Sciences*, *374*, 865–871.

Angelaki, D. E., & Hess, B. J. M. (1996). Three-dimensional organization of otolith-ocular reflexes in rhesus monkeys. I. Linear acceleration responses during off-vertical axis rotation. *Journal of Neurophysiology*, *75*, 2405–2424.

Böhmer, A., Henn, V., & Suzuki, J. I. (1985). Vestibulo-ocular reflexes after selective plugging of the semicircular canals in the monkey — response plane determinations. *Brain Research*, *326*, 291–298.

Bruno, P., & van den Berg, A. V. (1997). Relative orientation of primary positions of the two eyes. *Vision Research*, *7*, 935–947.

Cabungcal, J. H., Misslisch, H., Scherberger, S., Hepp, K., Hess, B. J. M. (2000). The effect of drowsiness on Listing's plane during static ocular counter-roll and counter-pitch in the monkey. Society for Neuroscience Abstract (in press).

Crawford, J. D., & Vilis, T. (1991). Axes of eye rotation and Listing's law during rotation of the head. *Journal of Neurophysiology*, *65*, 407–423.

Crawford, J. D., & Vilis, T. (1992). Symmetry of oculomotor burst neuron coordinates about Listing's plane. *Journal of Neurophysiology*, *68*, 432–448.

Crawford, J. D., & Vilis, T. (1999). Role of the primate 3D neural integrator in ocular counterroll during head tilt. *Society for Neuroscience Abstract*, *25*, 6.

Crawford, J. D., Cadera, W., & Vilis, T. (1991). Generation of torsional and vertical eye position signals by the interstitial nucleus of Cajal. *Science*, *252*, 1551–1553.

Demer, J. L., Miller, J. M., Poukens, V., Vinters, H. V., & Glasgow, B. J. (1995). Evidence for fibromuscular pulleys of the recti extraocular muscles. *Investigative Ophthalmology and Visual Science*, *36*, 1125–1136.

Demer, J. L., Poukens, V., Miller, J. M., & Micevych, P. (1997). Innervation of extraocular pulley smooth muscle in monkeys and humans. *Investigative Ophthalmology and Visual Science*, *38*, 1774–1785.

Demer, J. L., Oh, S. Y., & Poukens, V. (2000). Evidence for active control of rectus extraocular muscle pulleys. *Investigative Ophthalmology and Visual Science*, *41*, 1280–1290.

Efron, B., & Tibshirani, R. J. (1993). *An introduction to the bootstrap*. New York: Chapman and Hall.

Haslwanter, T., Straumann, D., Hess, B. J. M., & Henn, V. (1992). Static roll and pitch in the monkey: shift and rotation of Listing's plane. *Vision Research*, *32*, 1341–1348.

Haustein, W. (1989). Considerations on Listing's law and primary position by means of a matrix description of eye position control. *Biological Cybernetics*, *60*, 411–420.

Helmchen, C., Rambold, H., Fuhry, L., & Büttner, U (1998). Deficits in vertical and torsional eye movements after uni- and bilateral muscimol inactivation of the interstitial nuclues of Cajal of the alert monkey. *Experimental Brain Research*, *119*, 436–452.

Helmholtz, H. (1867). *Handbuch der Physiologischen Optik*. *Hamburg: Voss*. Third edition translated into English by J.P.C. Southall (1925) as Treatise on physiological optics. Optical Society of America, Rochester, NY.

Henn, V., Baloh, R. W., & Hepp, K. (1984). The sleep-wake transition in the oculomotor system. *Experimental Brain Research*, *54*, 166–176.

Henn, V., Straumann, D., Hess, B. J. M., Hepp, K., Vilis, T., & Reisine, H. (1991). Generation of vertical and torsional rapid eye movement in the rostral mesencephalon. Experimental data and clinical implications. *Acta Otolaryngologica*, *481*, 191–193.

Hess, B. J. M., Van Opstal, A. J., Straumann, D., & Hepp, K. (1992). Calibration of three-dimensional eye position using search coil signals in the rhesus monkey. *Vision Research*, *9*, 1647–1654.

Iwamoto, Y., Kitama, T., & Yoshida, K. (1990). Vertical eye movement-related secondary vestibular neurons ascending in medial longitudinal fasciculus in cat I. Firing properties and projection pathways. *Journal of Neurophysiology*, *64*, 902–917.

Kuhlo, W., & Lehman, D. (1964). Das Einschlaferleben und seine neurophysiologischen Korrelate. *Archiv für Psychiatrische Nervenkrankheiten*, *205*, 687–716.

Markham, C. H. (1989). Anatomy and physiology of otolith-controlled ocular counter-rolling. *Acta Otolaryngologica*, *468*, 263–266.

McCrea, R. A., Strassman, A., & Highstein, S. M. (1987). Anatomical and physiological characteristics of vestibular neurons mediating the vertical vestibulo-ocular reflexes of the squirrel monkey. *Journal of Comparative Neurology*, *4*, 471–494.

Miller, J. M., & Demer, J. L. (1997). New orbital constraints on eye rotation. In M. Fetter, T. Haslwanter, H. Misslisch, & D. Tweed, *Three-dimensional kinematic principles of eye, head and limb movements* (pp. 349–357). Amsterdam: Harwood.

Minken, A. W., & van Gisbergen, J. A. (1994). A three-dimensional analysis of vergence movements at various levels of elevation. *Experimental Brain Research*, *101*, 331–345.

Misslisch, H., & Hess, B. J. M. (1999). Effect of vergence on Listing's plane in rhesus monkey. *Society for Neuroscience Abstract*, *25*, 1400.

Misslisch, H., & Hess, B. J. M. (2000). Three-dimensional vestibulo-ocular reflex of the monkey: optimal gaze stabilization versus Listing's law. *Journal of Neurophysiology*, *83*, 3264–3276.

Misslisch, H., Tweed, D., Fetter, M., Sievering, D., & Koenig, E. (1994). Rotational kinematics of the human vestibulo-ocular reflex III. Listing's law. *Journal of Neurophysiology*, *72*, 2490–2502.

Mok, D., Ro, A., Cadera, W., Crawford, J. D., & Vilis, T. (1992). Rotation of Listing's plane during vergence. *Vision Research*, *32*, 2055–2064.

Nakayama, K. (1975). Coordination of extraocular muscles. In G. Lennerstrand, & P. Bach-y-Rita, *Basic mechanisms of ocular motility and their clinical implications* (pp. 193–209). Oxford: Pergamon.

van Opstal, A. J., Hepp, K., Suzuki, Y., & Henn, V. (1996). Role of monkey nucleus reticularis tegmenti pontis in stabilization of Listing's plane. *Journal of Neuroscience*, *22*, 7284–7296.

Press, W. H., Teukolsky, S. A., Vetterling, W. T., & Flannery, B. P. (1992). *Numerical recipes in C*. New York: Cambridge.

Raybourn, M. S., & Keller, E. L. (1977). Colliculoreticular organization in primate oculomotor system. *Journal of Neurophysiology*, *40*, 861–878.

Suzuki, Y., Straumann, D., Hess, B. J. M., & Henn, V. (1994). Changes of Listing's plane under physiological and pathological conditions. In J. M. Delgado-Garcia, E Godaux, & P. P. Vidal, *Information processing underlying gaze control* (pp. 75–86). Oxford: Pergamon.

Suzuki, Y., Büttner-Ennever, J. A., Straumann, D., Hepp, K., Hess, B. J. M., & Henn, V. (1995). Deficits in torsional and vertical rapid eye movements and shift of Listing's plane after uni- and bilateral lesions of the rostral interstitial nucleus of the medial longitudinal fasciculus (riMLF). *Experimental Brain Research*, *106*, 215–232.

Suzuki, Y., Kase, M., Kato, H., & Fukushima, K. (1997). Stability of ocular counter-rolling and Listing's plane during static roll-tilts. *Investigative Ophthalmology and Visual Science*, *38*, 2103–2111.

Straumann, D., Zee, D. S., & Solomon, D. (2000). Three-dimensional kinematics of ocular drift in humans with cerebellar atrophy. *Journal of Neurophysiology*, *83*, 1125–1140.

Tweed, D. (1997). Visual-motor optimization in binocular control. *Vision Research*, *37*, 1939–1951.

Tweed, D., & Vilis, T. (1990). Geometric relations of eye position and velocity vectors during saccades. *Vision Research*, *30*, 111–127.

Tweed, D., Fetter, M., Andreadaki, S., Koenig, E., & Dichgans, J. (1992). Three-dimensional properties of human pursuit eye movement. *Vision Research*, *32*, 1225–1238.

Wasicky, R., Ziya-Ghazvhini, F., Blumer, R., Lukas, J. R., & Mayr, R. (2000). Muscle fiber types of human extraocular muscles: a histochemical and immunohistochemical study. *Investigative Ophthalmology and Visual Science*, *5*, 980–990.